Journal of Chromatography B 1188 (2022) 123014

Contents lists available at ScienceDirect

Journal of Chromatography B

journal homepage: www.elsevier.com/locate/jchromb

Selective extraction of gambierone and related metabolites in *Gambierdiscus silvae* using *m*-aminophenylboronic acid–agarose gel and liquid chromatography–high-resolution mass spectrometric detection

Elizabeth M. Mudge [a,*], Alison Robertson [b,c], Alexander K. Leynse [b,c], Pearse McCarron [a], Christopher O. Miles [a]

[a] Biotoxin Metrology, National Research Council Canada, 1411 Oxford Street, Halifax, NS, B3H 3Z1, Canada
[b] Department of Marine Sciences, University of South Alabama, 5871 University Drive North, Mobile, AL 36688, United States
[c] Marine Ecotoxicology, Dauphin Island Sea Lab, Dauphin Island, Dauphin Island, AL 36528, United States

ARTICLE INFO

Keywords:
Gambierdiscus
LC-HRMS
Ciguatera
Boronic acid gel
Gambierone
vic-diol

ABSTRACT

Gambierdiscus spp. are epi-benthic dinoflagellates that have been associated with ciguatera poisoning. These microalgae can have complex secondary metabolite profiles including ciguatoxins, maitotoxins, and gambierones, with varying compositions and toxicities across species and strains. Given this chemical diversity there is a need to develop selective and sensitive methods for secondary metabolite profiling. In this study, we used a cultured Caribbean strain of *Gambierdiscus silvae* to develop sample preparation and analysis strategies for characterizing *vic*-diol containing secondary metabolites. A pooled cellular extract was first screened by liquid chromatography–high-resolution mass spectrometry (LC–HRMS) for ciguatoxin-related compounds, which resulted in the confirmation of gambierone (**1**) and a novel isomer of 44-methylgambierone (**3**). Treatment of the extract with periodate confirmed that the gambierones each contained one reactive *vic*-diol, which was exploited for the development of a selective extraction procedure using *m*-aminophenylboronic acid gel and the non-aqueous binding solvent chloroform. Using this non-traditional boronate affinity procedure, LC–HRMS also revealed the presence of additional sulfated polycyclic ethers in the gambierone-containing *vic*-diol fraction, while pigments and other contaminants were removed. The developed tools could be applied to screen collections of *Gambierdiscus* and other benthic algae to provide additional chemical characterization of gambierone-related compounds. The selective extraction procedure may also prove useful as a step in the isolation of these sulfated polyethers for structural, toxicological and biotransformation studies.

1. Introduction

Epi-benthic dinoflagellates growing on the surfaces of macroalgae and coral may be present as complex communities and may include *Gambierdiscus, Ostreopsis, Prorocentrum, Amphidinium* and *Coolia* spp., among many others [1,2]. Isolates of *Gambierdiscus* from Polynesia have been shown to produce a variety of algal precursors of ciguatoxins (CTXs) and are considered the causative agents of ciguatera poisoning in Pacific regions. Many additional *Gambierdiscus* and *Fukuyoa* spp. have been shown to have CTX-like activity, although the causative compounds are yet to be identified [3–10]. These dinoflagellates produce complex mixtures of metabolites with varying toxicities that can accumulate in grazing invertebrates and fish [11–14]. Ciguatera poisoning poses a significant public health risk to local coastal communities in tropical and subtropical regions, and globally with increasing trade and travel worldwide [15,16].

Gambierdiscus spp. produce a wide array of ladder-shaped polyether compounds including CTXs, maitotoxins (MTXs), gambierol, gambieric acids, gambierones (**1**–**3**; Fig. 1) and gambieroxide [17–24]. The varied distribution of these compounds among *Gambierdiscus* species and strains is likely a contributing factor for the different reported toxicities [25–27]. CTXs in contaminated fish that have been associated with ciguatera outbreaks were traditionally classified based on regional origin, and those that have been elucidated have structural distinctions (Fig. 1). Naming conventions that exclude regional prevalence have been proposed based on other marine and freshwater biotoxin classes

* Corresponding author at: National Research Council of Canada, 1411 Oxford Street, Halifax, NS Canada.
E-mail address: Elizabeth.mudge@nrc-cnrc.gc.ca (E.M. Mudge).

https://doi.org/10.1016/j.jchromb.2021.123014
Received 30 April 2021; Received in revised form 19 October 2021; Accepted 28 October 2021
Available online 2 November 2021

[28]. For instance, CTXs such as CTX1B (**4**), CTX3C (**5**) and CTX4B (**6**) originally detected in the Pacific have backbone structures containing 13 ether rings, with **5** containing an additional carbon at the E-ring relative to **4** and **6**. CTX1B is currently considered the most potent (and most studied) CTX and accumulates in fish muscle tissue following metabolism of the algal precursor CTX4B (**6**). CTXs originally observed in the Caribbean (e.g., C-CTX1, **7**) contain 14 ether rings which share structural similarities with **5** from rings B to J. C-CTX1 is considered less toxic than CTX1B [29], however more data is needed to verify toxicity equivalence. The algal precursors to C-CTXs have not yet been determined and as such, very little is known about the contribution and linkage of algal C-CTX metabolites to those reported in higher trophic levels. To date, the reported Indian Ocean CTXs have not yet been structurally elucidated [30,31]. To identify the precursors of these CTXs, appropriate analytical screening methods for algal metabolites are required. While many existing methods for evaluating the composition of *Gambierdiscus* spp. use targeted LC–MS [26,27], untargeted approaches with high resolution mass spectrometry can provide additional data pertaining to minor analogues and novel metabolites, including elemental formula predictions using exact masses and isotope distributions [32,33].

Algal extracts are complex, containing many secondary metabolites and potential matrix interferences that can hinder metabolite screening for potential phycotoxins. Many marine algal toxins contain *vic*-diols in their structures, including many CTXs, MTXs and gambierones. This structural characteristic has been exploited by procedures using polymer-bound boronic acids to selectively bind *vic*-diol containing compounds including glycoproteins [34], catecholamines [35] and more recently marine toxins [36,37]. Applications for clean-up of shellfish extracts containing azaspiracids and tetrodotoxins have highlighted this technique as a selective method for sample concentration and for reducing interferences and signal suppression in LC–MS analysis [36,37].

The aim of this work was to develop tools to facilitate screening of *Gambierdiscus* extracts for gambierones and related metabolites. Using liquid chromatography–high-resolution mass spectrometry (LC–HRMS), an extract of *Gambierdiscus silvae* was observed to contain gambierones and other sulfated polycyclic ethers, but no reported CTXs. Treatment with periodate was used to confirm the presence of 1,2-diols in the structures and a selective fractionation procedure was developed using a polymer-bound boronic acid. The resulting gambierone-enriched extract was profiled by LC–HRMS to reveal the presence of several novel putative sulfated polyethers in the extract, one of which was tentatively identified as 29-methylgambierone by analysis of its HRMS/MS spectra.

2. Material and methods

2.1. Chemicals and reagents

Methanol, acetonitrile and formic acid (~98%) were LC–MS grade from Fisher Scientific (Ottawa, ON, Canada). Chloroform and dichloromethane were from Caledon Laboratories (Georgetown, ON, Canada). Reagent grade sodium metaperiodate (>99%), 0.22 µm PTFE spin filters, and *m*-aminophenylboronic acid–agarose (mAPBAG) aqueous gel suspension were from Millipore-Sigma (Oakville, ON, Canada). Distilled water was ultra-purified to 18.2 MΩ·cm using a Milli-Q water purification system (Millipore–Sigma). Gambierone (19.9 µg/mL in MeOH) was from CIFGA (Lugo, Spain) and 44-methylgambierone (25 µg/mL in MeOH) was from Cawthron Institute (Nelson, New Zealand) [17]. Standards were obtained for final structural verification of

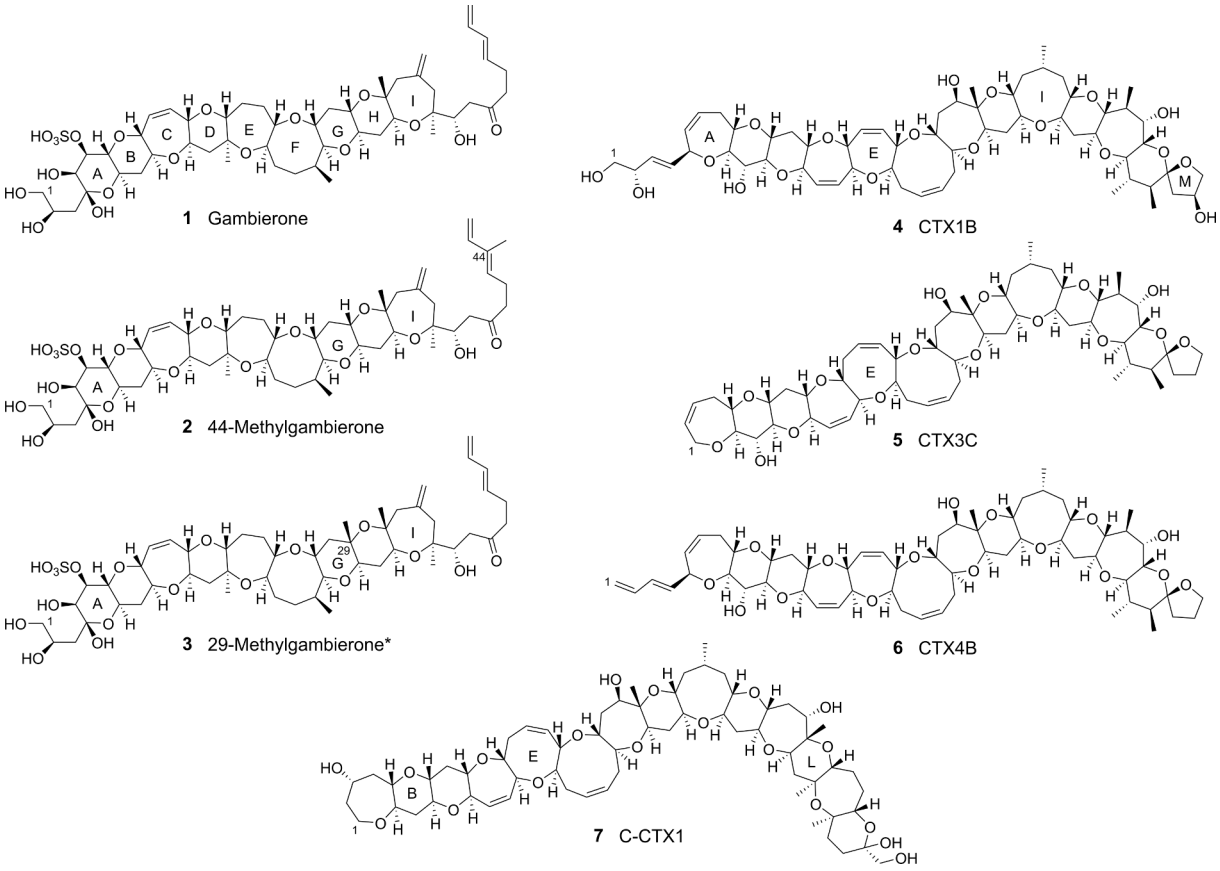

Fig. 1. Chemical structures of ladder-shaped polyethers associated with *Gambierdiscus* or fish related to ciguatera: gambierone (**1**), 44-methylgambierone (**2**), 29-methylgambierone (**3**), CTX1B (**4**), CTX3C (**5**), CTX4B (**6**) and C-CTX1 (**7**). *Note: novel methylgambierone tentatively identified in *G. silvae* (1504 FC-14) where the possibility of methylation at C-28 or C-30 cannot be excluded from the LC–HRMS/MS data.

the gambierones in the *G. silvae* extract.

2.2. G. Silvae culture maintenance

An established culture of *G. silvae* (1504 FC-14) was provided by Deana L. Erdner (University of Texas at Austin, TX, USA). This dinoflagellate was isolated from a sample collected from Flat Cay, St. Thomas, U.S. Virgin Islands (GPS 18.31822 N, −64.99104 W) in April 2015 and has been reported in prior studies [38]. Cultures were grown at 25 °C on a 12:12 h light:dark cycle in 50 mL borosilicate culture tubes containing 15 mL of medium. Irradiances during the light cycle were maintained at a photon flux of ~ 75 μmol/m^2/s. The culture medium was a modified version of the recipe from Keller *et al.*, (1987), in which Tris and silica were excluded [39]. Constituents of the Keller medium were added to artificial seawater prepared to a salinity of 36 ppt with Instant Ocean salts (Instant Ocean, Blacksburg, VA) and filter-sterilized through a 0.22 μm cellulose acetate filter (Millipore–Sigma, Burlington, MA).

Once culture densities in 15 mL of medium reached > 2,000 cell/mL, the culture was transferred to 500 mL of medium and placed underneath down-facing cool white fluorescent lamps with a constant photon flux of 75 μmol/m^2/s. Prior to harvest, 1.1 mL duplicate sub-samples were collected and preserved with 1% (v/v) glutaraldehyde. To estimate culture cell density, 1 mL of each of the glutaraldehyde-preserved sub-samples was loaded onto a Sedgewick Rafter counting chamber. Counts from each sample were converted to cell densities in cells/mL. Cell density estimates from duplicate sub-samples were averaged and then multiplied by the total culture volume to estimate total cells per culture. Additional, non-preserved, subsamples (30 μL) were collected and immediately observed under the microscope to confirm typical cell morphology, flagellar movement, and behavior as proxies for culture health.

2.3. Sample preparation

G. silvae (1504 FC-14) was prepared in triplicate 500 mL cultures and concentrated to 50 mL by filtering onto 25 mm diameter, 20 μm pore size nylon mesh filters and then rinsing cells off the filter into 50 mL polypropylene centrifuge tubes with isotonic K medium. The 50 mL cell suspensions were then centrifuged (300 × *g* at 20 °C), the supernatants were carefully removed from each sample using a glass Pasteur pipette, and the pellets frozen and stored at −20 °C.

The cellular pellets from replicate cultures were pooled to maximize available material (representing in total 811,000 *G. silvae* cells) and extracted with MeOH (1.5 mL) containing 0.5 mL of 0.5 mm diameter glass beads using a Beadruptor24 (Omni International, Kennesaw, USA). Suspended cells were ruptured for 2 × 30 s with a 2 min cooldown period in-between. The extract was centrifuged (2,600 × *g* at 20 °C) and the supernatant was removed. Remaining cellular debris and glass beads were rinsed twice with MeOH (1.5 mL), centrifuged (2,600 × *g*), and the MeOH rinses were combined with the supernatant. The extract was transferred to a 250 mL separatory funnel and diluted to 30 mL with MeOH. The extract was adjusted to 60% MeOH by the addition of deionized H_2O (20 mL) and partitioned with CH_2Cl_2 (3 × 20 mL). The CH_2Cl_2 extracts were pooled and evaporated at 40 °C via rotary evaporation. The resulting residue was dissolved in MeOH (1 mL) and diluted 10-fold with MeOH for LC–HRMS analysis and periodate reactions.

2.4. Treatment with sodium periodate

An aliquot (95 μL) of the diluted *G. silvae* extract was mixed with aqueous sodium metaperiodate ($NaIO_4$) (5 μL, 50 mM). A control sample was prepared by adding water (5 μL) to the diluted extract (95 μL). The samples were vortex-mixed (30 s) and placed in the HPLC autosampler. The control sample was analyzed at time zero, followed by the IO_4^--treated sample at 2 h intervals for 12 h.

2.5. Selective fractionation with m-aminophenylboronic acid-agarose gel

The mAPBAG (200 μL) was prepared by filtering on a PTFE spin filter (0.45 μm; Canada Life Science, Peterborough, ON, Canada) to remove the liquid medium and washing sequentially with MeOH and $CHCl_3$ (100 μL each) prior to use. The wash solvents were removed by filtration with a PTFE spin filter (0.45 μm). An aliquot (20 μL) of the undiluted *G. silvae* extract was evaporated under a gentle stream of N_2 at 25 °C in a 2 mL vial. The residue was dissolved in $CHCl_3$ (500 μL) and the prepared mAPBAG was added. The vial was maintained at ambient temperature on a Multitherm shaker (Mandel Scientific, Guelph, ON, Canada) at 850 rpm for 3 h. The suspension was filtered on a PTFE spin filter (0.45 μm) to remove the chloroform, an aliquot (100 μL) of the chloroform was evaporated under N_2, and the residue dissolved in MeCN–H_2O (1:1 v/v, 100 μL). The mAPBAG was returned to the vial and residual solvent removed from the gel with a gentle flow of N_2. The gel was extracted with MeCN–H_2O (1:1, 500 μL) at ambient temperature in the shaker at 850 rpm for 2 h, and the solution filtered (0.45 μm PTFE). A control sample of the undiluted *G. silvae* extract was prepared by evaporating 20 μL under N_2 and dissolving the residue in MeCN–H_2O (1:1, 500 μL).

2.6. LC–HRMS analysis

Analyses were performed using an Agilent 1200 LC equipped with a binary pump, temperature controlled autosampler (10 °C) and temperature-controlled column compartment (40 °C) (Agilent Technologies, Missisauga, ON, Canada) coupled to a Q Exactive HF Orbitrap mass spectrometer (Thermo Fischer Scientific, Waltham, MA, USA) with a heated electrospray ionization probe (HESI-II). Chromatographic separation was on a Kinetex 1.7 μm F5 pentafluorophenyl column (100 × 2.1 mm, Phenomenex, Torrance, CA, USA) using gradient elution with mobile phases composed of 0.1% formic acid in H_2O (A) and 0.1% formic acid in MeCN (B). The gradient was: 0–18 min, 10–80 % B; 18–18.1 min, 80–99 % B; 18.1–22 min, 99 %B; followed by an 8 min re-equilibration at 10% B, with a flow rate of 0.3 mL/min and an injection volume of 5.0 μL.

Full-scan acquisition was performed with positive and negative polarity switching with a mass range of *m/z* 700–1400 to target potential polyethers present in the *G. silvae* extract. A second full scan acquisition with a high-mass-range scan was performed from *m/z* 1250–3500 to evaluate the presence of high molecular weight MTXs. The spray voltage of the source was +4500 V or −2500 V, with a capillary temperature of 340 °C. The sheath and auxiliary gas were set at 40 and 10 (arbitrary units). The probe heater temperature was set at 150 °C and the S-Lens RF level was set to 100. The mass resolution setting was 120,000 with an automatic gain control (AGC) target of 1 × 10^6 and a maximum injection time of 100 ms per scan.

Product-ion spectra were acquired using targeted parallel reaction monitoring (PRM) scan mode with an isolation window of 1 Da. The resolution setting was 60,000 with an AGC target of 5 × 10^6 and a maximum injection time of 512 ms with a collision energy of 30 or 45 eV in positive mode and normalized collision energy of 45 eV in negative mode. The exact masses evaluated are listed in Table S1. Scheduled PRM scans were performed for each ionization mode.

Molecular formula assignments were evaluated using XCalibur (Elemental Composition tab) with restrictions based on observations of in-source behavior in positive and negative modes. For peaks with in-source loss of SO_3 in positive ionization, the following constraints were used: Carbon: 0–70; Hydrogen: 0–125; Oxygen: 0–25; Sulfur: 1; ring plus double bond equivalents (RDBE): 5–100; a mass tolerance of 5 ppm, and; a charge of 1. Isotope distribution calculations were performed with the NRC Molecular Formula Calculator (2021; v1.1, https://metrology.shinyapps.io/molecular-formula-calculator/) previously used for microcystin analysis, which bases the calculations on the accurate masses and relative intensities of the isotopomer peaks observed in the pseudo-molecular ions acquired in full-scan HRMS and

the natural abundance of isotopes [40].

3. Results and discussion

3.1. LC–HRMS analysis of G. Silvae (1504 FC-14)

An untargeted LC–HRMS method was used to screen the composition of the *Gambierdiscus* extract. A method originally developed for C-CTXs [41] was adapted in-house with a wider gradient to detect metabolites with a wide degree of polarities that may be present in the extract. The total ion chromatograms for both positive and negative modes are shown in Fig. 2. A manual mass search of the high and low mass acquisitions, with a mass tolerance of 5 ppm, was performed against an in-house database containing exact masses of pseudo molecular ions and adduct ions of known *Gambierdiscus*-related compounds including MTXs, gambieric acids, gambierones, and CTXs reported from the Pacific and Caribbean. A summary of the compounds included in the search and their corresponding exact masses are summarized in Table S2. Due to the ever expanding knowledge on the geographical range and prevalence of *Gambierdiscus* species [42,43], all reported *Gambierdiscus*-related compounds, regardless of geographical region, were examined. The extract did not contain detectable levels of any previously reported CTXs, including the C-CTX variants reported in fish [41]. However, two peaks with accurate masses matching known compounds were observed. The first peak was consistent with gambierone (**1**; $[M + H]^+$ *m/z* 1025.4751, $C_{51}H_{77}O_{19}S^+$, Δ −2.3 ppm), and the retention time, full-scan spectra, and product ion spectra of **1** matched those of the gambierone standard (Figures S2 and S3). The second peak **3** ($[M + H]^+$ *m/z* 1039.4914, $C_{52}H_{79}O_{19}S^+$, Δ −1.6 ppm) had an accurate mass matching 44-methylgambierone (**2**), however, the retention time and product ion spectra did not match the standard (Figures S4 and S5), suggesting that **3** could be an isomer of 44-methylgambierone (**2**). Gambierones readily fragment in the source, as shown in the full-scan mass spectra of **1** and **3** in Fig. 3. Water losses, in addition to the apparent loss of SO_3 from the presumed pseudomolecular ion, are observed which is consistent with sulfated polycyclic ethers. A small peak at 12.0 min had an accurate mass consistent with gambierone (*m/z* 1025.4779; $C_{51}H_{77}O_{19}S^+$, Δ 0.5 ppm) in positive ionization, but upon further investigation did not have gambierone-like properties based on in-source and MS/MS behavior.

To determine the probable structure of **3**, and to verify its identity as a gambierone, the MS/MS spectrum of **1** was first evaluated in detail to identify characteristic cleavages and diagnostic product ions. The fragment-rich $[M + H]^+$ product ion spectrum of gambierone in Fig. 4 proved structurally informative for this sulfated polycyclic ether, whereas the $[M - H]^-$ product ion spectrum provided limited structural information, with the major product ion of *m/z* 96.9601 (HSO_4^-; Δ 0.0 ppm) confirming this is a sulfated molecule (Figure S6). In positive mode with a CE of 45 eV, neutral loss of SO_3 (at C-6) occurred readily and was not present in any of the ions observed (Fig. 4). Up to nine water losses from each product ion added additional complexity to the spectra. The MS/MS fragment nomenclature described for C-CTX 3/4 [41] is used here to label the cleavages (s, p and q) observed within the polyether rings and are summarized in Table S3. The most abundant fragments were in the low mass range, including *m/z* 161.0960 ($C_{11}H_{13}O^+$, Δ −0.3 ppm), and 219.1378 ($C_{14}H_{19}O_2^+$, Δ −0.6 ppm) where the *m/z* 219 product ion is consistent with previous findings [19,44]. These correspond to cross-ring cleavages of the I-ring between C-36/C-37 with a loss of water, and C-34/C-35, respectively. The product ion at *m/z* 803.4209 ($C_{43}H_{63}O_{14}^+$, Δ −0.3 ppm) is from cleavage between C-38 and C-39 with a water loss from *m/z* 821.4313 ($C_{43}H_{65}O_{15}^+$, Δ −0.6 ppm). While product ions from loss of water and SO_3 from the pseudomolecular ion, and low mass fragments at *m/z* 109.0647 ($C_7H_{13}O^+$, Δ −0.7 ppm) and *m/z* 81.0698 ($C_6H_9^+$, Δ −0.9 ppm), are consistent with previous studies [17,19,44,45], they do not provide the structural evidence for the polyether backbone necessary for the tentative identification of **3**.

Lower abundance product ions from the cleavage of rings E–I were observed. The cleavage between the I-ring and the hydroxyketone aliphatic chain (q_9) was observed with *m/z* 751.3899 ($C_{39}H_{59}O_{14}^+$, Δ −1.1 ppm). Fragmentation on the right side of the polyether bonds (p, q') were the predominant product ions observed, together with their respective water losses. The product ions observed at *m/z* 567.2782

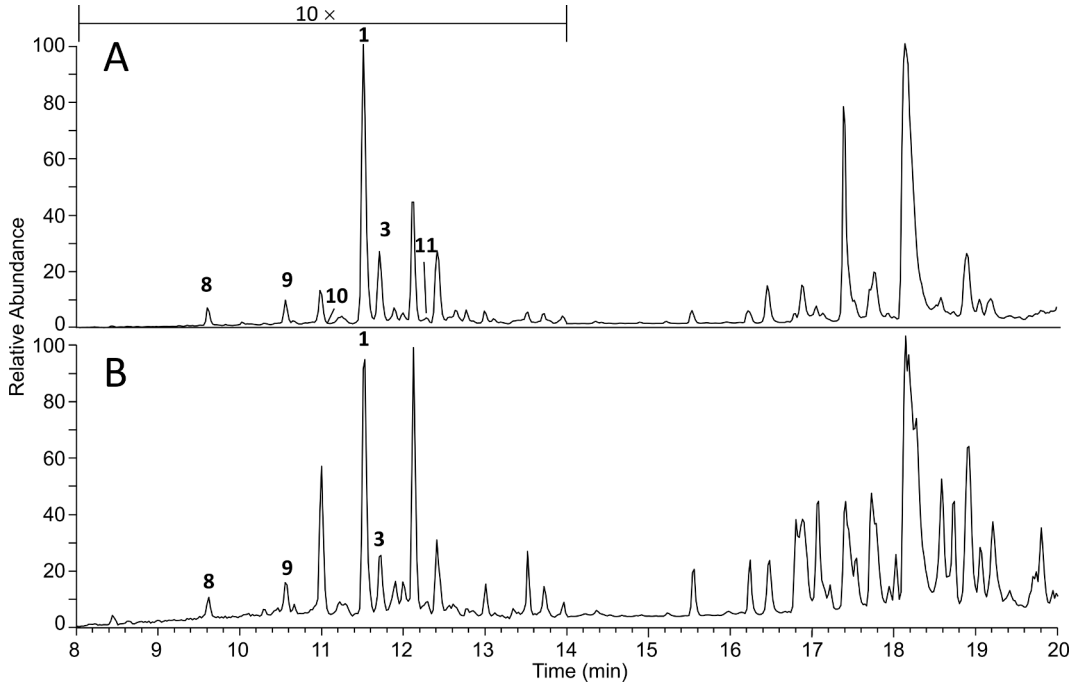

Fig. 2. Total ion chromatograms (*m/z* 700–1400) of *G. silvae* (1504 FC-14) extract using LC–HRMS with: (A) negative ionization, and; (B) positive ionization. The compound numbers label gambierones and other peaks observed subsequently in the mAPBAG gel fraction. The vertical scale from 8 to 14 min was expanded 10-fold to highlight these peaks. For a full-scale chromatogram, see Figure S1.

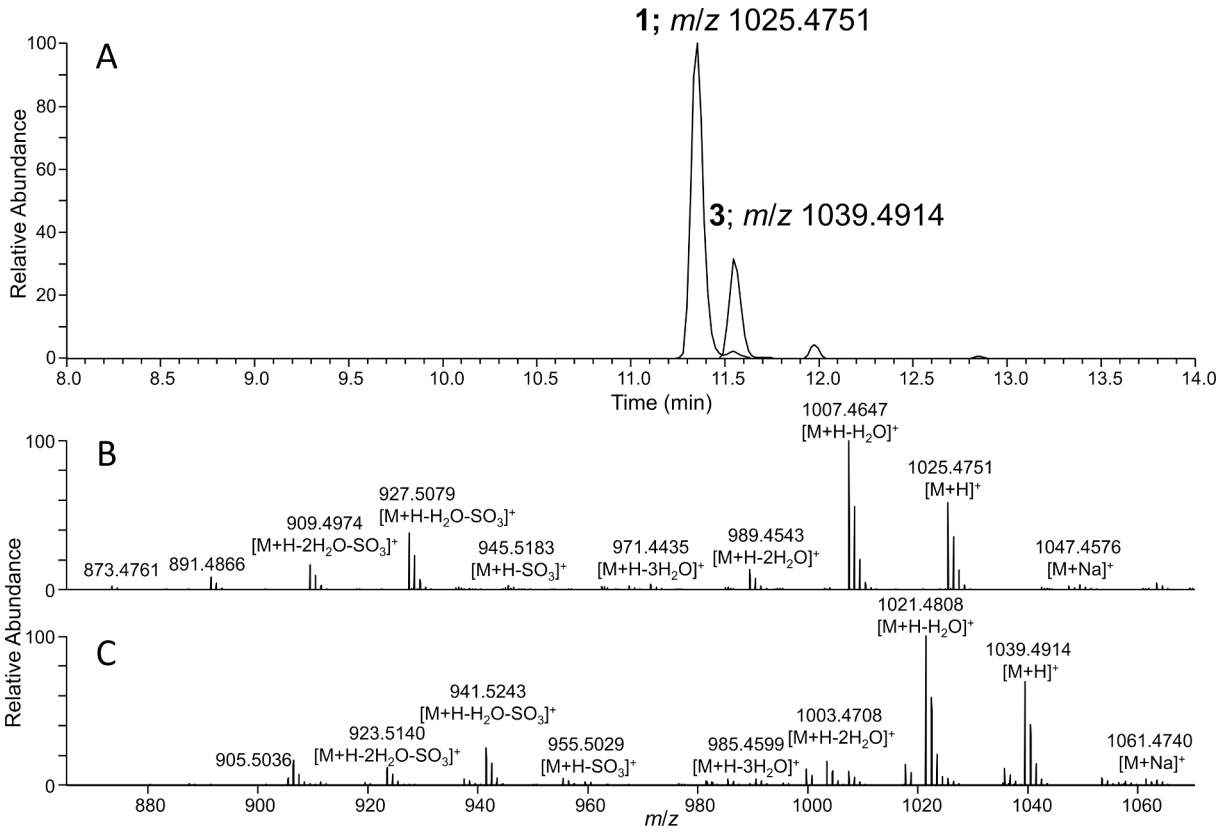

Fig. 3. (A) Extracted ion LC–HRMS chromatogram of *m/z* 1025.4774 and 1039.4931 (±5 ppm) of *G. silvae* (1504 FC-14) in positive mode and their respective full-scan spectra with in-source fragmentation (B, C). The pseudomolecular ions matched the known *Gambierdiscus* metabolites gambierone (**1**) and a methylgambierone, later tentatively identified as 29-methylgambierone (**3**).

($C_{29}H_{43}O_{11}^+$, Δ −3.2 ppm) and *m/z* 549.2685 ($C_{29}H_{41}O_{10}^+$, Δ −1.8 ppm) are consistent with the p_6 cleavage and its water loss, respectively, while *m/z* 623.3054 ($C_{32}H_{47}O_{12}^+$, Δ −1.3 ppm) and *m/z* 693.3479 ($C_{36}H_{53}O_{13}^+$, Δ –1.0 ppm) are consistent with p_7 and p_8 cleavages. The right-side fragments of these cleavages were also observed (q'_2 and q'_3 with water losses) at *m/z* 303.1953 ($C_{19}H_{27}O_3^+$, Δ –0.5 ppm) and *m/z* 341.2109 ($C_{22}H_{29}O_3^+$, Δ –0.8 ppm), respectively. The relative abundance of product ions between *m/z* 300 and 450 is lower in comparison with these other product ions, although the cleavage between rings E and F (s_5) at *m/z* 457.2071 ($C_{22}H_{33}O_{10}^+$, Δ 0.6 ppm) was observed. The cleavage between rings F and G was observed with the loss of 4 water molecules ($s_5 - 4H_2O$) at *m/z* 485.2525 ($C_{28}H_{37}O_7^+$, Δ –1.8 ppm).

The product ion spectrum of $[M + H]^+$ of **3** resulted in neutral loss of SO_3 and multiple water losses from the pseudomolecular ion (Fig. 5). **2** has an additional methyl group at C-44 on the aliphatic chain side of the molecule, relative to **1**, with a signature fragment [19,45] at *m/z* 233.1533 (Figure S5). The major product ions of **3** in the low mass region were identical to those observed for **1** including a product ion at *m/z* 219.1378 (rather than at *m/z* 233.1533, as in **2**), indicating that this compound contains the same I-ring and unsaturated hydroxyketone-containing aliphatic chain as **1**. Product ions from cleavages p8 and p7 in **3** indicate that the additional methyl group (relative to **1**) is still present, and therefore is present on rings A–G, while cleavages at s_6 and p_6 are identical to those observed in **1**. These product ions, at *m/z* 485.2526 ($C_{26}H_{37}O_7^+$, Δ −1.6 ppm) and *m/z* 549.2691 ($C_{29}H_{41}O_{10}^+$, Δ −0.6 ppm), suggest that rings A–F of **3** are identical to those in **1**, and therefore that the additional methyl group of **3** is located between the G-and H-rings. Comparison of the product ion spectra of **1** and **3** are summarized in Table S3 and Figure S7. The exact location of the methyl group cannot be definitively assigned using mass spectrometry, but the experimental data localized the methylation between C-28 and C-30. The finding that both **1** and **3** are produced by *G. silvae* (1504 FC-14) suggests that these metabolites are produced through the same biosynthetic pathway, and would be expected to contain the same backbone structure and stereochemistry. Visual comparison of gambierones (Fig. 1) indicates that methylation on non-terminal six-membered rings occurs at ring junctions. This suggests that methylation is likely to be at C-29 or C-30. When adjacent six-membered polyether rings are methylated, the majority are methylated on the same side of the molecule, further suggesting that methylation will most likely occur at C-29, and **3** is therefore tentatively identified as 29-methylgambierone (Fig. 5). Confirmation of the site of methylation awaits isolation and analysis by NMR spectroscopy. This previously unreported analogue confirms the presence of constitutional isomers of 44-methylgambierone produced by some *Gambierdiscus* species [46], and suggests that further diversity among the gambierone family can be expected in this genus.

3.2. Time course for oxidation of the G. Silvae extract with sodium periodate

Reaction with sodium periodate was used to determine the presence of compounds containing 1,2-diols in the *G. silvae* extract, in a similar manner to that used recently in the identification of C-CTXs [41]. Gambierone contains a terminal 1,2-diol at C-1 and C-2, for which periodate cleavage will result in the loss of 32.0262 Da (Fig. 6) [17]. The reaction was monitored at 2-hour intervals for 12 h to determine the reactivity of the gambierones in the extract. Periodate cleavage of **1** was confirmed by the loss of 32.0262 Da upon oxidation, and was also observed for **3**, with the product eluting approximately 0.4 min later (Fig. 6). Plots of the peak areas of **1** and **3** and their respective periodate

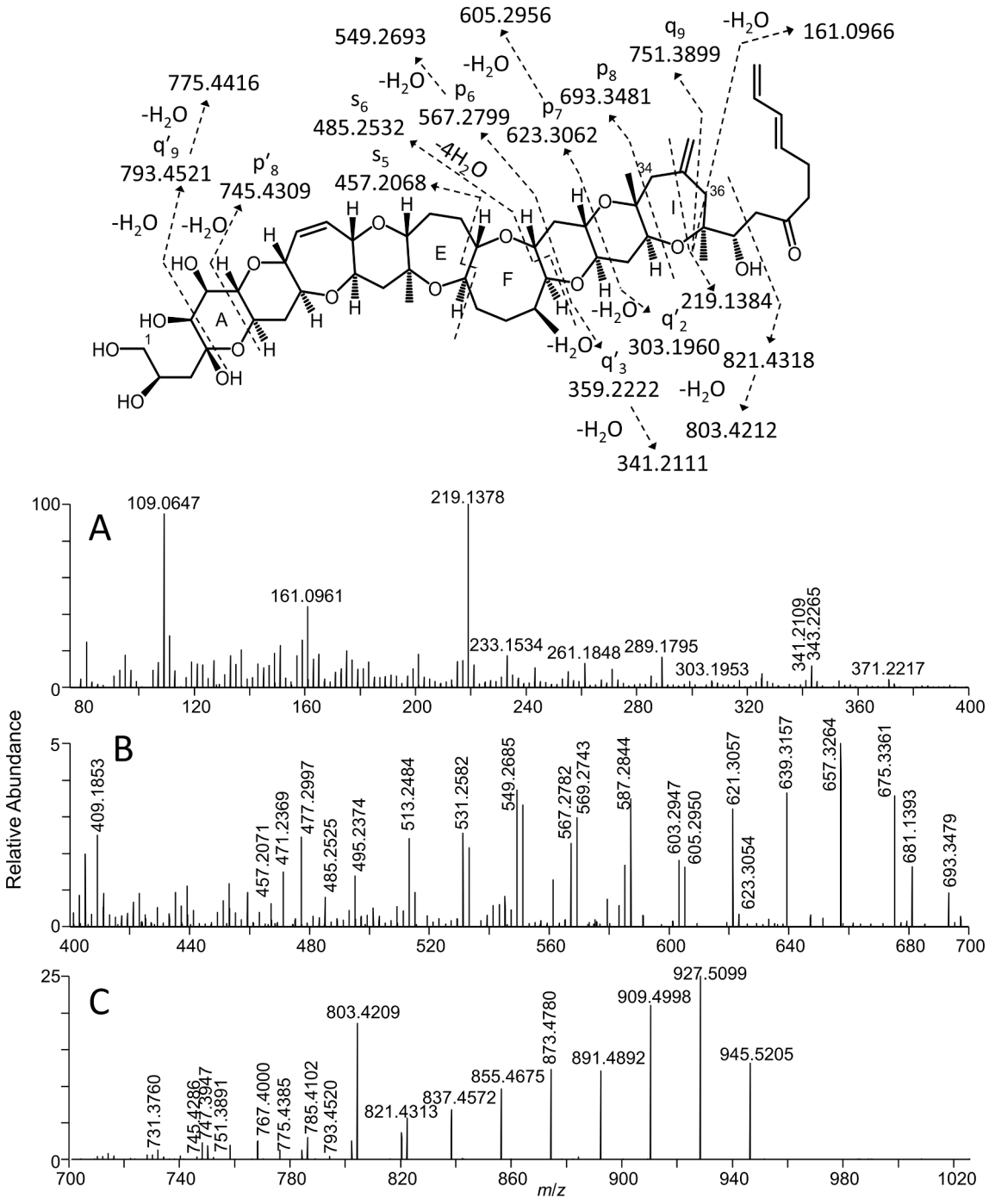

Fig. 4. Product ion spectrum of gambierone (**1**) ($[M + H]^+$ *m/z* 1025.4774) in positive ion mode using a collision energy of 45 eV, with the main fragments depicted on the structure $[M + H - SO_3]^+$: (A) mass range from *m/z* 75–400; (B) mass range from *m/z* 400–700, and; (C) mass range from *m/z* 700–1025.

oxidation products over time are shown in Figure S8. Periodate was added to the algal extract containing both **1** and **3**, where these two metabolites both reacted in the same solution and under identical conditions. Under these conditions, the time-course of the periodate oxidation reactions of **1** and **3** were identical, indicating that the diols in **1** and **3** are chemically very similar and located at the same region of the molecule. Taken together with the mass spectral data, this confirms that **3** contains a terminal diol at C-1 and C-2. Approximately 75% of the peaks observed in the LC–HRMS chromatogram of the *G. silvae* extract reacted with periodate within 12 h, with numerous new peaks appearing, indicating that many compounds in the extract contain 1,2-diols (Figure S9).

3.3. Fractionation of gambierones with m-aminophenyl boronic acid gel

The presence of 1,2-diols on the gambierones made them candidates for selective fractionation using immobilized boronic acids. Several commercially available immobilized boronic acid gels were tested including boric acid gel, polymer bound boronic acid (both Millipore–Sigma), immobilized boronic acid gel (Thermo Fisher Scientific), and mAPBAG. The mAPBAG provided the best recovery and was used for further investigations. Boronic acid gel clean-up procedures take advantage of the reversible binding between the diols and the boronic acid that has been covalently bound to a solid support (gel) and can subsequently be released by adjusting the solvent conditions [47,48].

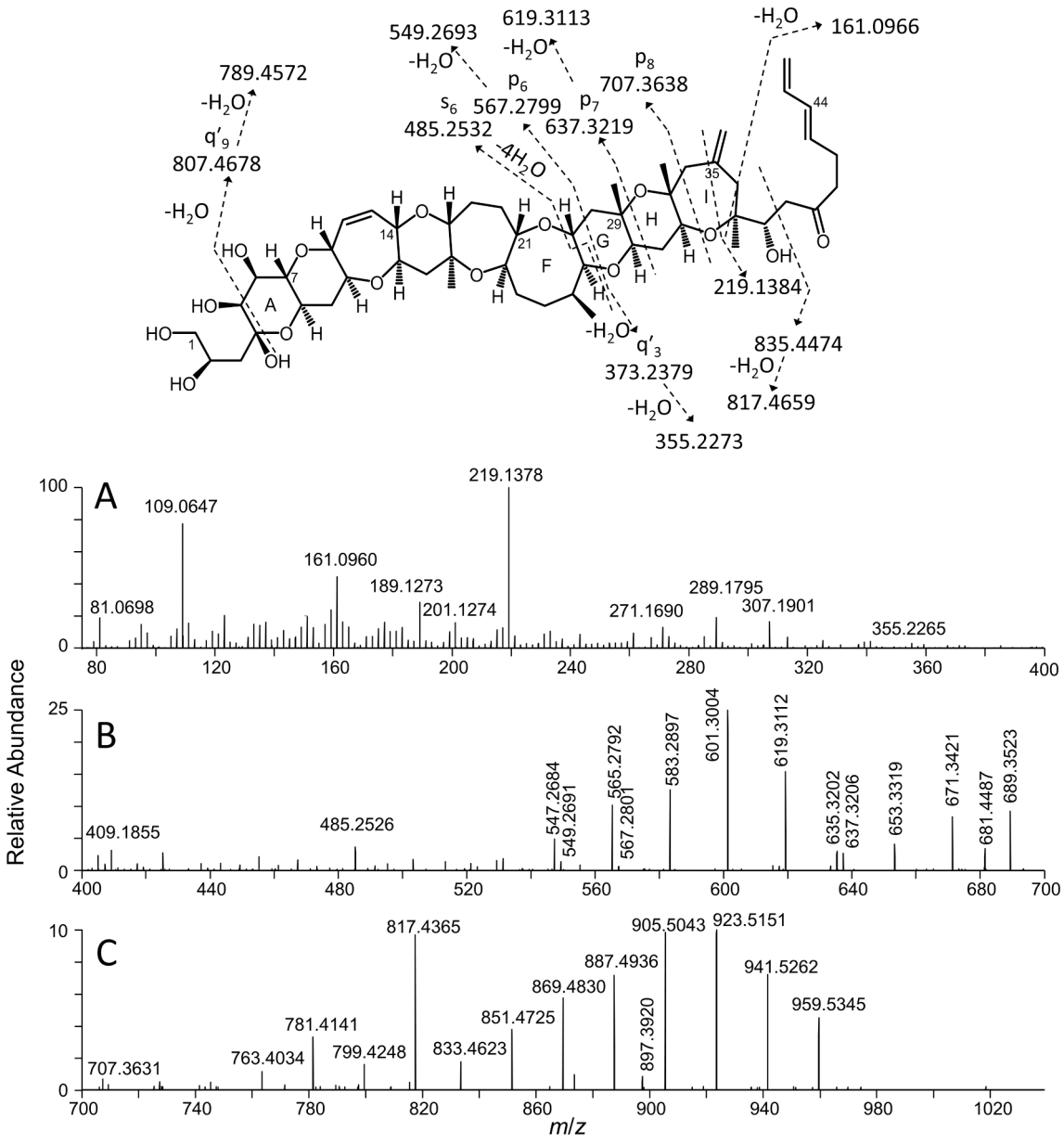

Fig. 5. Product ion spectrum of putative 29-methylgambierone (**3**) ($[M + H]^+$ *m/z* 1039.4931) in positive mode using a collision energy of 45, showing the proposed structure $[M + H - SO_3]^+$ and origins of the diagnostic product ions. (A) Mass range from *m/z* 75–400; (B) from *m/z* 400–700, and; (C) from *m/z* 700–1040.

Traditional boronic acid–diol complexation occurs using basic conditions, followed by release in acidic conditions [37,48]. While some success was obtained using basic complexation and acidic release for the gambierones in the *G. silvae* extract, lower binding and recovery of the gambierones was observed, together with the presence of pigments in the gambierone fraction. This behavior may be due to the presence of a primary alcohol in the diol of **1** making it more difficult to form a boronate complex under aqueous conditions [48], therefore a number of non-aqueous binding conditions were tested. Successful conditions developed for gambierone fractionation utilized a dispersive SPE technique by preparing a suspension of the mAPBAG with the algal extract in $CHCl_3$, requiring 3 h for complete binding. Dispersive SPE provided significant improvement in metabolite binding compared to loading the mAPBAG using a conventional SPE cartridge procedure due to the longer exposure time between the extract and gel. The $CHCl_3$ solution was removed and the gel was recovered. The gambierones were released from the gel using a solution of 1:1 (v/v) MeCN–H_2O for 2 h. Comparison of the control, chloroform and released eluate fractions (Fig. 7, S10) indicated that many components of the sample extract were selectively bound by the gel and subsequently released. The original extract had a slight yellow–orange color which, when applied to the gel, remained in the chloroform solution. The elution solvent was nearly colorless, indicating successful removal of most pigments in the extract (Fig. 7). Peak area comparisons of the control, chloroform and eluate fractions indicated > 97% of **1** and **3** bound to the gel, with average recoveries of **1** and **3** around 105% in the final eluate. Visual comparison of the chromatograms shows that several peaks eluting near gambierone remained in the $CHCl_3$ fraction (Fig. 7, S10), indicating that the higher recovery may due to reduced matrix interferences.

Several isomers of the known [49] algal carotenoid P457 ($[M + H]^+$ *m/z* 941.5242, $C_{52}H_{77}O_{15}^+$, Δ −1.6 ppm) were tentatively identified in the *G. silvae* extract based on exact mass and product ion spectra (Figure S11). These pigments reacted with periodate to produce later-eluting peaks with a loss of H_2, suggesting the diol cleavage occurred in the sugar ring, producing two aldehydes on the terminal sugar moiety (Figure S11). Given that these pigments were present in the mAPBAG

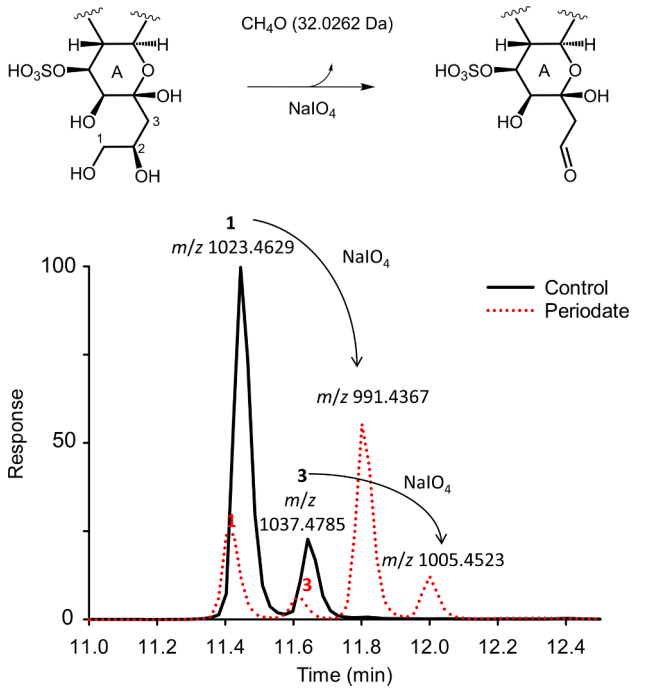

Fig. 6. Scheme summarizing the cleavage of the terminal diol at C-1 and C-2 on the A-ring of **1** and **3** following periodate treatment, and extracted ion LC–HRMS chromatograms of gambierone (**1**) and putative 29-methylgambierone (**3**) present in *G. silvae* (1504 FC-14) before (black line) and after (red dashed line) 12-h treatment with periodate, showing periodate cleavage products observed from loss of 32.0262 Da in negative ionization mode.

eluate when employing the traditional basic conditions for binding diols, followed by release in acidic conditions, but did not bind with the mAPBAG when employing the chloroform binding conditions, suggests that there is selective binding of certain diols including those found in gambierones using this non-traditional fractionation method.

3.4. Additional sulfated metabolites in the mAPBAG gambierone fraction

Several additional peaks were observed by LC–HRMS in the mAPBAG eluate, suggesting they possess similar chemical properties to gambierones. Compound **8** eluted at 9.6 min with $[M + H]^+$ *m/z* 929.4559 in positive ionization mode and was assigned a molecular formula of $C_{46}H_{73}O_{17}S^+$ (RDBE 11, Δ −0.4 ppm). Another compound eluted at 10.6 min (**9**) with $[M + H]^+$ *m/z* 941.4548 was assigned a probable molecular formula of $C_{47}H_{73}O_{17}S^+$ (RDBE 12, Δ −1.6 ppm). Both peaks showed in-source behavior characteristic of sulfated polyethers including water losses and loss of SO_3 (Fig. 8). Two later-eluting peaks at 11.1 and 12.1 min were observed in the mAPBAG fraction but were only detected in negative mode, with $[M - H]^-$ at *m/z* 1051.4594 and 995.4699 (**10** and **11**, respectively) with potential molecular formulae of $C_{52}H_{75}O_{20}S^-$ (RDBE 15, Δ 2.1 ppm) and $C_{50}H_{75}O_{18}S^-$ (RDBE 13, Δ 2.9 ppm). Comparison of the observed and calculated isotope distribution patterns for the pseudomolecular ions of **10** and **11** (as well as for **1**, **3**, **8** and **9**) and their proposed molecular formulae are summarized in Figure S12. MS/MS fragmentation for these metabolites in negative mode produced a major product at *m/z* 96.9601 (HSO_4^-; Δ 0.0 ppm). The molecular formulae, high RDBE, facile in-source fragmentation, and major product ions at *m/z* 96.9601 in negative mode all suggested these to be sulfated polyether compounds. Product ion spectra in positive mode for **8** and **9** (Figure S13) showed the loss of SO_3 and up to seven additional water losses from the pseudomolecular ions, but

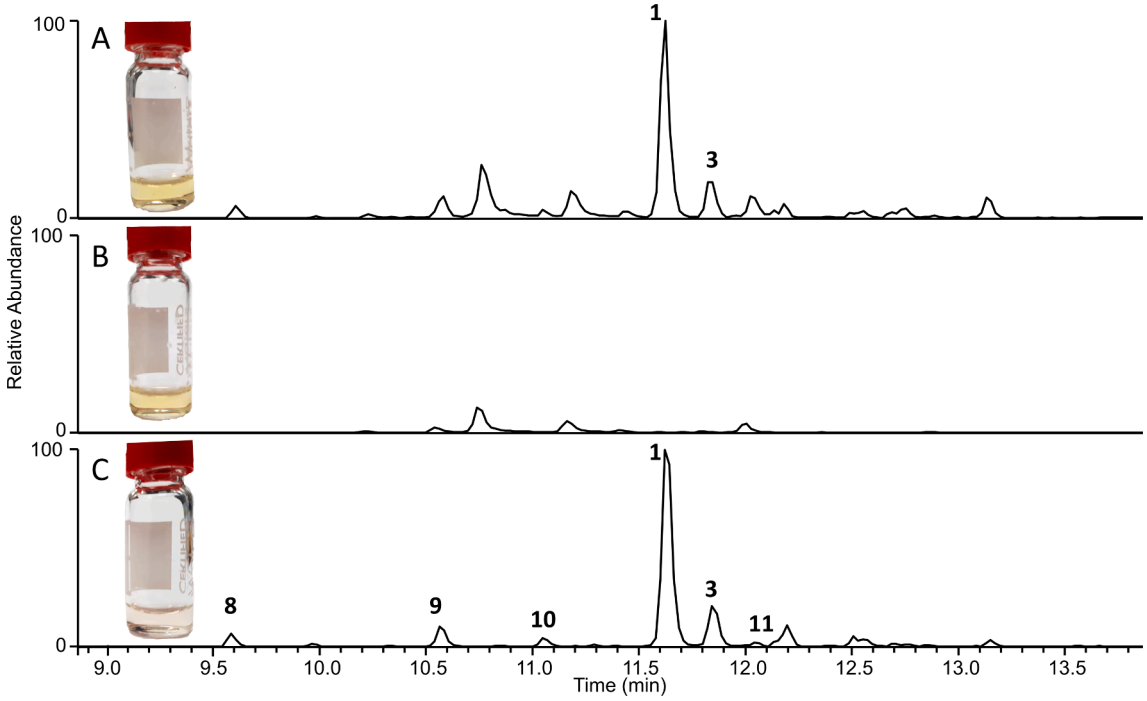

Fig. 7. Base-peak chromatograms from 9 to 14 min in negative ionization mode from *m/z* 750–1400 of the *G. silvae* extract before and after clean-up with mAPBAG. (A) Control; (B) $CHCl_3$ fraction (components not captured by the gel), and; (C) components released from the gel with 1:1 (v/v) MeCN–H_2O. The vertical scale for each chromatogram is the maximum peak intensity observed in the control. For a full-scale chromatogram, see Figure S10.

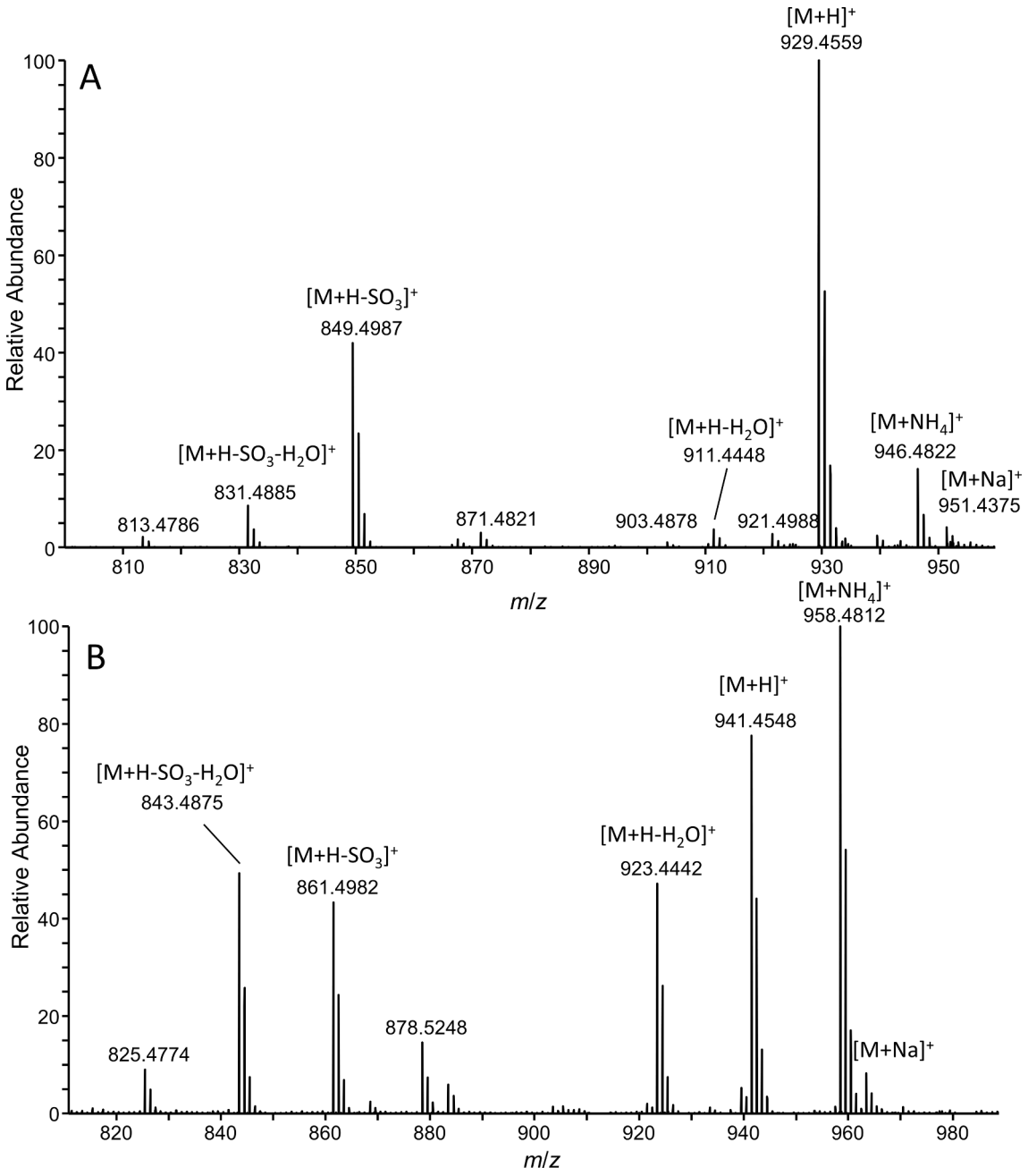

Fig. 8. (A) Full-scan mass spectra (positive ionization mode) of: **8**, a probable sulfated polycyclic ether with $[M + H]^+$ at *m/z* 929.4579 and probable molecular formula of $C_{46}H_{73}O_{17}S^+$, and; (B) **9**, a probable sulfated polycyclic ether with $[M + H]^+$ at *m/z* 941.4548 with potential molecular formula of $C_{47}H_{73}O_{17}S^+$.

there were no clear gambierone-diagnostic fragments observed, such as those for the hydroxyketone aliphatic chain at *m/z* 219.1381 or *m/z* 233.1533. This suggests the structures of these metabolites vary from gambieriones but they may be intermediates in the biosynthetic pathways. The structure elucidation of these metabolites was not pursued further as part of this work, but warrant future investigation to establish their biosynthetic and toxicological significance relative to gambierones in *Gambierdiscus* extracts.

The periodate reactivity of these additional metabolites in the gambierone-enriched mAPBAG fraction was monitored throughout the 12 h reaction. Approximately 20–25% of **8**, **9** and **10** reacted with periodate over 12 h, but no products with the loss of 32.0262 Da were observed. However, **11** most likely has a terminal 1,2-diol, as it reacted at a similar rate to gambierones **1** and **3**, with approximately 75% reacted after 12 h and a potential product formed from the loss of 32.0262 Da ($[M - H]^-$ at *m/z* 964.4437). This suggests that **8**, **9** and **10** contain diols in less reactive positions than **1**. Table 1 summarizes the properties of the compounds observed in the mAPBAG fraction. The product ion spectra, reactivity with periodate and behavior with boronic acid complexation of these metabolites further suggest they possess some properties similar to gambierones, although structural differences were observed.

This work identified the presence of gambierones and several potentially gambierone-like metabolites present in the CH_2Cl_2 fraction of a *G. silvae* extract. Recent studies have reported that the majority of gambierones remain in the methanolic fraction obtained during liquid–liquid partitioning between CH_2Cl_2 and MeOH–water [44], which suggests that there may be additional gambierones or sulfated

Table 1
Summary of the properties of the compounds observed in the gambierone enriched fraction from the mAPBAG fractionation procedure of the extract of *G. silvae* (1504 FC-14).

Compound #	Retention time (min)	Accurate Mass $[M+H]^+$ or $[M-H]^-$	Molecular Formula[a]	RDBE	HSO_4^- product in negative MS/MS	% Reacted with $NaIO_4$ after 12 h	$NaIO_4$ product −32.0262 Da
1	11.6	1025.4751	$C_{51}H_{76}O_{19}S$	14	Yes	75	Yes
3	11.7	1039.4923	$C_{52}H_{78}O_{19}S$	14	Yes	75	Yes
8	9.6	929.4559	$C_{46}H_{72}O_{17}S$	11	Yes	25	No
9	10.6	941.4548	$C_{47}H_{72}O_{17}S$	12	Yes	25	No
10	11.1	(-) 1051.4594	$C_{52}H_{76}O_{20}S$	15	Yes	20	No
11	12.1	(-) 995.4699	$C_{50}H_{76}O_{18}S$	13	Yes	75	Yes

[a] Neutral formula

polyethers produced by this species that were not evaluated in this study. Future work will focus on the application of this HRMS screening method and selective extraction techniques on crude extracts of *Gambierdiscus*, to establish its applicability to a broader range of metabolites and to evaluate its ability to remove additional matrix components in these extracts.

A number of bioassays have been developed to assess CTX and MTX activity [50,51]. Ciguatoxins act as sodium channel activators, while MTXs, specifically the large polyether maitotoxin-1 (MTX-1), activate calcium channels leading to an increase in the cytosolic Ca^{2+} ions [5,51–53]. These assays have been used extensively to screen *Gambierdiscus* spp., where ciguatoxic activity varies considerably between species and strains. Reports have indicated that several species have ciguatoxic activity, with *G. excentricus* exhibiting the highest CTX-like activity across several collections [8,9,51]. *G. silvae* tends to have above average ciguatoxic effects when compared to other *Gambierdiscus* spp. [8,9,51] and was selected for establishing these complementary methodologies to screen for potential toxins. The production of a gambierone-enriched fraction from this species as described herein could be used to help determine the toxicological significance of these metabolites, and these tools could also be applied to profile additional species.

Current knowledge on the biotransformation, accumulation and depuration of toxins responsible for ciguatera focuses primarily on the CTXs originally detected in Pacific regions. The algal CTXs, CTX3C and CTX4A/B, that have been detected in some species of *Gambierdiscus*, are oxidized in fish to metabolites such as 2,3-dihydroxyCTX3C and CTX1B, as confirmed through *in vitro* liver microsome and *in vivo* fish feeding studies [12,54]. These investigations have relied on research identifying the original algal precursors, for which backbone structures of the metabolites are shared between the precursors and the fish metabolites. To date, the algal precursors responsible for Caribbean CTXs have yet to be identified. However, based on knowledge related to biotransformations of CTX4A/B and CTX3C, it would be expected that the algal precursors share similar backbone structures to the fish metabolites.

Although gambierone and methylgambierones do not share backbone structures with characterized CTXs, they have been shown to have similar *in vitro* bioactivities to CTX3C, but with much lower potencies, thus having CTX-like rather than MTX-like activity [18,19]. Recent findings suggest that purified 44-methylgambierone has relatively low toxicity using mouse bioassays [55], which suggests that additional metabolites or potential synergistic toxicities of components may be present in crude *Gambierdiscus* extracts. Additionally, MTX-1 accumulation in fish flesh has been observed, suggesting that sulfated polyethers may also accumulate in fish flesh [56]. The majority of screening methods employed to date for *Gambierdiscus* cultures involve targeted MS/MS screening for known CTXs. Given that many cultures of *Gambierdiscus* have been found to be negative for CTX precursors, it is hypothesized that a different suite of toxin precursors are present. The high resolving power of high-resolution mass spectrometry provides the ability to screen wide mass ranges to highlight and potentially identify candidate peaks of interest. The ability to assign RDBE, molecular formula, perform targeted MS/MS fragmentation experiments, identify the presence of *vic*-diols, and to selectively extract these highlighted peaks from matrix components, provides capabilities for investigating these compounds and their potential for biotransformation to CTXs. While the algal precursors to C-CTXs are not yet known, these analyses and selective fractionation procedures can be used as tools for screening large *Gambierdiscus* collections in conjunction with bioassay screens to detect potential algal precursors.

4. Conclusions

LC–HRMS combined with periodate cleavage and boronic-acid-based fractionation of an extract of *G. silvae* 1504 FC-14, collected from the US Virgin Islands, revealed several gambierone-like

metabolites. Gambierone and a previously unreported methylgambierone isomer, tentatively identified as 29-methylgamberione, were detected in the extract. Reaction with periodate confirmed the presence of 1,2-diols in the structure of these metabolites, and this was exploited to selectively fractionate these metabolites using an immobilized boronic acid. Several additional sulfated polycyclic ethers were identified in the gambierone-enriched fraction from the boronic acid gel. Future research will focus on the application of these procedures to facilitate screening collections of *Gambierdiscus* in combination with bioassays to identify the toxicological significance of these fractions and potentially identify metabolites related to ciguatoxin accumulation in fish in the Caribbean Sea.

CRediT authorship contribution statement

Elizabeth M. Mudge: Methodology, Investigation, Visualization, Writing – original draft. **Alison Robertson:** Supervision, Writing – review & editing, Funding acquisition. **Alexander K. Leynse:** Investigation, Writing – original draft. **Pearse McCarron:** Supervision, Funding acquisition, Writing – review & editing. **Christopher O. Miles:** Conceptualization, Methodology, Funding acquisition, Writing – review & editing.

Declaration of Competing Interest

The authors declare that they have no known competing financial interests or personal relationships that could have appeared to influence the work reported in this paper.

Acknowledgments

The authors thank Tyler B. Smith and his team at the University of the Virgin Islands (St. Thomas, US Virgin Islands) for the collection of live algal material used in isolations, Deana L Erdner (University of Texas, Marine Sciences Institute (Port Aransas, Texas)) for *Gambierdiscus* culture establishment and sequence identification, and D. Tim Harwood, Michael J. Boundy, and J. Sam Murray (Cawthron Institute, Nelson, New Zealand) for an in-house standard of 44-methylgambierone.

This work was funded in part by the National Science Foundation (NSF) Partnerships in International Research and Education Program (CiguaPIRE; 1743802) and contributes to the NSF and NIEHS Center for Oceans and Human Health: Greater Caribbean Center for Ciguatera Research (NSF: 1841811 and NIH: 1P01ES028949-01).

Appendix A. Supplementary data

Supplementary data to this article can be found online at https://doi.org/10.1016/j.jchromb.2021.123014.

References

[1] E.D. Irola-Sansores, B. Delgado-Pech, E. García-Mendoza, E.J. Núñez-Vázquez, A. Olivos-Ortiz, A. Almazán-Becerril, Population dynamics of benthic-epiphytic dinoflagellates on two macroalgae from coral reef systems of the Northern Mexican Caribbean, Front. Mar. Sci. 5 (2018) 487.

[2] M.L. Parsons, M.L. Richlen, A. Robertson, Harmful Algal Species Fact Sheet: *Gambierdiscus*, in: S.E. Shumway, J.M. Burkholder, S.L. Morton (Eds.), Harmful Algal Blooms, John Wiley & Sons, Hoboken, NJ, 2018, pp. 601–604.

[3] A.L. Kretzschmar, M.E. Larsson, M. Hoppenrath, M.A. Doblin, S.A. Murray, Characterisation of two toxic *Gambierdiscus* spp. (Gonyaulacales, Dinophyceae) from the Great Barrier Reef (Australia): *G. lewisii* sp. nov. and *G. holmesii* sp. nov. Protist 170 (2019) 125699.

[4] M.E. Larsson, T.D. Harwood, R.J. Lewis, M.A. Doblin, Toxicological characterization of *Fukuyoa paulensis* (Dinophyceae) from temperate Australia, Phycol. Res. 67 (2019) 65–71.

[5] M.E. Larsson, O.F. Laczka, D.T. Harwood, R.J. Lewis, S.W.A. Himaya, S.A. Murray, M.A. Doblin, Toxicology of *Gambierdiscus* spp. (Dinophyceae) from tropical and temperate Australian waters, Mar. Drugs 16 (2018) 7.

[6] L. Díaz-Asencio, M. Vandersea, N. Chomérat, S. Fraga, R.J. Clausing, R.W. Litaker, D. Chamero-Lago, M. Gómez-Batista, A. Moreira-González, P. Tester, C. Alonso-Hernández, M.-Y. Dechraoui Bottein, Morphology, toxicity and molecular characterization of *Gambierdiscus* spp. towards risk assessment of ciguatera in south central Cuba, Harmful Algae 86 (2019) 119–127.

[7] S. Fraga, F. Rodríguez, A. Caillaud, J. Diogène, N. Raho, M. Zapata, *Gambierdiscus excentricus* sp. nov. (Dinophyceae), a benthic toxic dinoflagellate from the Canary Islands (NE Atlantic Ocean), Harmful Algae 11 (2011) 10–22.

[8] R.W. Litaker, W.C. Holland, D.R. Hardison, F. Pisapia, P. Hess, S.R. Kibler, P. A. Tester, S. Lin, Ciguatoxicity of *Gambierdiscus* and *Fukuyoa* species from the Caribbean and Gulf of Mexico, PLoS ONE 12 (10) (2017), e0185776, https://doi.org/10.1371/journal.pone.018577610.

[9] E.A. Rossignoli, A. Tudó, I. Bravo, A.P. Díaz, J. Diogène, P. Riobó, Toxicity characterisation of *Gambierdiscus* species from the Canary Islands, Toxins 12 (2020) 134.

[10] M. Murata, A.M. Legrand, Y. Ishibashi, M. Fukui, T. Yasumoto, Structures and configurations of ciguatoxin from the moray eel *Gymnothorax javanicus* and its likely precursor from the dinoflagellate *Gambierdiscus toxicus*, J. Am. Chem. Soc. 112 (1990) 4380–4386.

[11] Y.L. Mak, T.-C. Wai, M.B. Murphy, W.H. Chan, J.J. Wu, J.C.W. Lam, L.L. Chan, P.K. S. Lam, Pacific ciguatoxins in food web components of coral reef systems in the Republic of Kiribati, Environ. Sci. Technol. 47 (2013) 14070–14079.

[12] T. Ikehara, K. Kuniyoshi, N. Oshiro, T. Yasumoto, Biooxidation of ciguatoxins leads to species-specific toxin profiles, Toxins 9 (2017) 205.

[13] H.T. Darius, M. Roué, M. Sibat, J. Viallon, C.M. Gatti, M.W. Vandersea, P.A. Tester, R.W. Litaker, Z. Amzil, P. Hess, M. Chinain, Toxicological investigations on the sea urchin *Tripneustes gratilla* (Toxopneustidae, Echinoid) from Anaho Bay (Nuku Hiva, French Polynesia): evidence for the presence of Pacific ciguatoxins, Mar. Drugs 16 (2018) 122.

[14] H.T. Darius, M. Roué, M. Sibat, J. Viallon, C.M. Gatti, M.W. Vandersea, P.A. Tester, R.W. Litaker, Z. Amzil, P. Hess, M. Chinain, *Tectus niloticus* (Tegulidae, Gastropod) as a novel vector of ciguatera poisoning: detection of Pacific ciguatoxins in toxic samples from Nuku Hiva Island (French Polynesia), Toxins 10 (2018) 2.

[15] M.A. Friedman, M. Fernandez, L.C. Backer, R.W. Dickey, J. Bernstein, K. Schrank, S. Kibler, W. Stephan, M.O. Gribble, P. Bienfang, R.E. Bowen, S. Degrasse, H. A. Flores Quintana, C.R. Loeffler, R. Weisman, D. Blythe, E. Berdalet, R. Ayyar, D. Clarkson-Townsend, K. Swajian, R. Benner, T. Brewer, L.E. Fleming, An updated review of ciguatera fish poisoning: clinical, epidemiological, environmental, and public health management, Mar. Drugs 15 (2017) 72.

[16] M. Chinain, C.M.i. Gatti, H.T. Darius, J.-P. Quod, P.A. Tester, Ciguatera poisonings: a global review of occurrences and trends, Harmful Algae 102 (2021), 101873, https://doi.org/10.1016/j.hal.2020.101873.

[17] J.S. Murray, A.I. Selwood, D.T. Harwood, R. van Ginkel, J. Puddick, L.L. Rhodes, F. Rise, A.L. Wilkins, 44-Methylgambierone, a new gambierone analogue isolated from *Gambierdiscus australes*, Tetrahedron Lett. 60 (2019) 621–625.

[18] I. Rodríguez, G. Genta-Jouve, C. Alfonso, K. Calabro, E. Alonso, J.A. Sánchez, A. Alfonso, O.P. Thomas, L.M. Botana, Gambierone, a ladder-shaped polyether from the dinoflagellate *Gambierdiscus belizeanus*, Org. Lett. 17 (2015) 2392–2395.

[19] A. Boente-Juncal, M. Álvarez, Á. Antelo, I. Rodríguez, K. Calabro, C. Vale, O. P. Thomas, L.M. Botana, Structure elucidation and biological evaluation of maitotoxin-3, a homologue of gambierone, from *Gambierdiscus belizeanus*, Toxins 11 (2019) 79.

[20] A. Morohashi, M. Satake, H. Nagai, Y. Oshima, T. Yasumoto, The absolute configuration of gambieric acids A–D, potent antifungal polyethers, isolated from the marine dinoflagellate *Gambierdiscus toxicus*, Tetrahedron 56 (2000) 8995–9001.

[21] E.P. Mazzola, J.R. Deeds, W.L. Stutts, C.D. Ridge, R.W. Dickey, K.D. White, R. T. Williamson, G.E. Martin, Elucidation and partial NMR assignment of monosulfated maitotoxins from the Caribbean, Toxicon 164 (2019) 44–50.

[22] M.J. Holmes, R.J. Lewis, Purification and characterisation of large and small maitotoxins from cultured *Gambierdiscus toxicus*, Nat. Toxins 2 (1994) 64–72.

[23] M. Satake, M. Murata, T. Yasumoto, Gambierol: a new toxic polyether compound isolated from the marine dinoflagellate *Gambierdiscus toxicus*, J. Am. Chem. Soc. 115 (1993) 361–362.

[24] R. Watanabe, H. Uchida, T. Suzuki, R. Matsushima, M. Nagae, Y. Toyohara, M. Satake, Y. Oshima, A. Inoue, T. Yasumoto, Gambieroxide, a novel epoxy polyether compound from the dinoflagellate *Gambierdiscus toxicus* GTP2 strain, Tetrahedron 69 (2013) 10299–10303.

[25] L. Rhodes, T. Harwood, K. Smith, P. Argyle, R. Munday, Production of ciguatoxin and maitotoxin by strains of *Gambierdiscus australes*, *G. pacificus* and *G. polynesiensis* (Dinophyceae) isolated from Rarotonga, Cook Islands, Harmful Algae 39 (2014) 185–190.

[26] K. Roeder, K. Erler, S. Kibler, P. Tester, H. Van The, L. Nguyen-Ngoc, G. Gerdts, B. Luckas, Characteristic profiles of ciguatera toxins in different strains of *Gambierdiscus* spp. Toxicon 56 (2010) 731–738.

[27] J.S. Murray, M.J. Boundy, A.I. Selwood, D.T. Harwood, Development of an LC–MS/MS method to simultaneously monitor maitotoxins and selected ciguatoxins in algal cultures and P-CTX-1B in fish, Harmful Algae 80 (2018) 80–87.

[28] Food and Agriculture Organization of the United Nations, World Health Organization, Report of the expert meeting on ciguatera poisoning: Rome, 19–23 November 2018, World Health Organization, Rome, 2020. https://apps.who.int/iris/handle/10665/332640.

[29] J.P. Vernoux, R.J. Lewis, Isolation and characterisation of Caribbean ciguatoxins from the horse-eye jack (*Caranx latus*), Toxicon 35 (1997) 889–900.

[30] J. Diogène, L. Reverté, M. Rambla-Alegre, V. del Río, P. de la Iglesia, M. Campàs, O. Palacios, C. Flores, J. Caixach, C. Ralijaona, I. Razanajatovo, A. Pirog, H. Magalon, N. Arnich, J. Turquet, Identification of ciguatoxins in a shark involved in a fatal food poisoning in the Indian Ocean, Sci. Rep. 7 (2017) 8240.

[31] B. Hamilton, M. Hurbungs, A. Jones, R.J. Lewis, Multiple ciguatoxins present in Indian Ocean reef fish, Toxicon 40 (2002) 1347–1353.
[32] P. Blay, J.P.M. Hui, J. Chang, J.E. Melanson, Screening for multiple classes of marine biotoxins by liquid chromatography–high-resolution mass spectrometry, Anal. Bioanal. Chem. 400 (2011) 577–585.
[33] J. Qiu, C. Rafuse, N.I. Lewis, A. Li, F. Meng, D.G. Beach, P. McCarron, Screening of cyclic imine and paralytic shellfish toxins in isolates of the genus *Alexandrium* (Dinophyceae) from Atlantic Canada, Harmful Algae 77 (2018) 108–118.
[34] B. Preinerstorfer, M. Lämmerhofer, W. Lindner, Synthesis and application of novel phenylboronate affinity materials based on organic polymer particles for selective trapping of glycoproteins, J. Sep. Sci. 32 (2009) 1673–1685.
[35] S. Higa, T. Suzuki, A. Hayashi, I. Tsuge, Y. Yamamura, Isolation of catecholamines in biological fluids by boric acid gel, Anal. Biochem. 77 (1977) 18–24.
[36] D.G. Beach, E.S. Kerrin, P. McCarron, J. Kilcoyne, S.D. Giddings, T. Waaler, T. Rundberget, I.A. Samdal, K.E. Løvberg, C.O. Miles, Boronate techniques for clean-up and concentration of the *vic*-diol-containing tetrodotoxins and azaspiracids from shellfish, in: P. Hess (Ed.), Harmful Algae 2018 – From Ecosystems to Socioecosystems, International Society for the Study of Harmful Algae, Nantes France, 2020, pp. 125–128.
[37] C.O. Miles, J. Kilcoyne, P. McCarron, S.D. Giddings, T. Waaler, T. Rundberget, I. A. Samdal, K.E. Løvberg, Selective extraction and purification of azaspiracids from blue mussels (*Mytilus edulis*) using boric acid gel, J. Agric. Food Chem. 66 (2018) 2962–2969.
[38] Y. Lozano-Duque, M.L. Richlen, T.B. Smith, D.M. Anderson, D.L. Erdner, Development and validation of PCR-RFLP assay for identification of *Gambierdiscus* species in the Greater Caribbean Region, J. Appl. Phycol. 30 (2018) 3529–3540.
[39] M.D. Keller, R.C. Selvin, W. Claus, R.R.L. Guillard, Media for the culture of oceanic ultraphytoplankton, J. Phycol. 23 (1987) 633–638.
[40] V. Mallia, S. Uhlig, C. Rafuse, J. Meija, C.O. Miles, Novel microcystins from *Planktothrix prolifica* NIVA-CYA 544 identified by LC-MS/MS, functional group derivatization and ^{15}N-labeling, Mar. Drugs 17 (2019) 643.
[41] F. Kryuchkov, A. Robertson, C.O. Miles, E.M. Mudge, S. Uhlig, LC–HRMS and chemical derivatization strategies for the structure elucidation of Caribbean ciguatoxins: identification of C-CTX-3 and -4, Mar. Drugs 18 (2020) 182.
[42] P. Tester, L. Wickliffe, J. Jossart, L. Rhodes, H. Envoldsen, M. Adachi, T. Nishimura, F. Rodriguez, M. Chinain, W. Litaker, Global distribution of the genera *Gambierdiscus* and *Fukuyoa*, in: P. Hess (Ed.), Harmful Algae 2018 - From Ecosystems to Socioecosystems, International Society for the Study of Harmful Algae, Nantes France, 2020, pp. 21–26.
[43] À. Tudó, A. Toldrà, M. Rey, I. Todolí, K.B. Andree, M. Fernández-Tejedor, M. Campàs, F.X. Sureda, J. Diogène, *Gambierdiscus* and *Fukuyoa* as potential indicators of ciguatera risk in the Balearic Islands, Harmful Algae 99 (2020), 101913.
[44] P. Estevez, M. Sibat, J.M. Leão-Martins, A. Tudó, M. Rambla-Alegre, K. Aligizaki, J. Diogène, A. Gago-Martinez, P. Hess, Use of mass spectrometry to determine the diversity of toxins produced by *Gambierdiscus* and *Fukuyoa* species from Balearic Islands and Crete (Mediterranean Sea) and the Canary Islands (Northeast Atlantic), Toxins 12 (2020) 305.
[45] C.E. Tibiriçá, M. Sibat, L.F. Fernandes, G. Bilien, N. Chomérat, P. Hess, L. L. Mafra Jr, Diversity and toxicity of the Genus *Coolia* Meunier in Brazil, and detection of 44-methyl gambierone in *Coolia tropicalis*, Toxins 12 (2020) 327.
[46] F. Pisapia, M. Sibat, C. Herrenknecht, K. Lhaute, G. Gaiani, P.-J. Ferron, V. Fessard, S. Fraga, S.M. Nascimento, R.W. Litaker, W.C. Holland, C. Roullier, P. Hess, Maitotoxin-4, a novel MTX analog produced by *Gambierdiscus excentricus*, Mar. Drugs 15 (2017) 220.
[47] G. Springsteen, B. Wang, A detailed examination of boronic acid–diol complexation, Tetrahedron 58 (2002) 5291–5300.
[48] D.G. Hall, Structure, properties, and preparation of boronic acid derivatives. Overview of their reactions and applications, in: D.G. Hall (Ed.), Boronic Acids: Preparation and Applications in Organic Synthesis and Medicine, Wiley-VCH, Weinheim, 2005, pp. 1–99.
[49] G. Englert, T. Aakemann, K. Schiedt, S. Liaaen-Jensen, Structure elucidation of the algal carotenoid (3*S*,5*R*,6*R*,3′*S*,5′*R*,6′*S*)-13′-*cis*-7′,8′-dihydroneoxanthin-20′-al 3′-β-lactoside (P457). Part 2, NMR studies, J. Nat. Prod. 58 (1995) 1675–1682.
[50] A. Caillaud, H. Eixarch, P. de la Iglesia, M. Rodriguez, L. Dominguez, K.B. Andree, J. Diogène, Towards the standardisation of the neuroblastoma (neuro-2a) cell-based assay for ciguatoxin-like toxicity detection in fish: application to fish caught in the Canary Islands, Food Addit. Contam. 29 (2012) 1000–1010.
[51] F. Pisapia, W.C. Holland, D.R. Hardison, R.W. Litaker, S. Fraga, T. Nishimura, M. Adachi, L. Nguyen-Ngoc, V. Séchet, Z. Amzil, C. Herrenknecht, P. Hess, Toxicity screening of 13 *Gambierdiscus* strains using neuro-2a and erythrocyte lysis bioassays, Harmful Algae 63 (2017) 173–183.
[52] M.-Y. Dechraoui, J. Naar, S. Pauillac, A.-M. Legrand, Ciguatoxins and brevetoxins, neurotoxic polyether compounds active on sodium channels, Toxicon 37 (1999) 125–143.
[53] G.M. Nicholson, R.J. Lewis, Ciguatoxins: cyclic polyether modulators of voltage-gated ion channel function, Mar. Drugs 4 (2006) 82–118.
[54] J. Li, Y.L. Mak, Y.-H. Chang, C. Xiao, Y.-M. Chen, J. Shen, Q. Wang, Y. Ruan, P.K. S. Lam, Uptake and depuration kinetics of Pacific ciguatoxins in orange-spotted grouper (*Epinephelus coioides*), Environ. Sci. Technol. 54 (2020) 4475–4483.
[55] J.S. Murray, T. Nishimura, S.C. Finch, L.L. Rhodes, J. Puddick, D.T. Harwood, M. E. Larsson, M.A. Doblin, P. Leung, M. Yan, F. Rise, A.L. Wilkins, M.R. Prinsep, The role of 44-methylgambierone in ciguatera fish poisoning: acute toxicity, production by marine microalgae and its potential as a biomarker for *Gambierdiscus* spp, Harmful Algae 97 (2020), 101853.
[56] G.S. Kohli, G.G. Papiol, L.L. Rhodes, D.T. Harwood, A. Selwood, A. Jerrett, S. A. Murray, B.A. Neilan, A feeding study to probe the uptake of maitotoxin by snapper (*Pagrus auratus*), Harmful Algae 37 (2014) 125–132.